Stickiness: A New Variable to Characterize the Temperature and Humidity Contributions toward Humid Heat

CATHERINE C. IVANOVICH,[a] ADAM H. SOBEL,[a,b,c] RADLEY M. HORTON,[b] AND COLIN RAYMOND[d,e]

[a] *Earth and Environmental Sciences, Columbia University, New York, New York*
[b] *Lamont-Doherty Earth Observatory, Columbia University, Palisades, New York*
[c] *Applied Physics and Applied Mathematics, Columbia University, New York, New York*
[d] *University of California, Los Angeles, Los Angeles, California*
[e] *Jet Propulsion Laboratory/California Institute of Technology, Pasadena, California*

(Manuscript received 15 April 2023, in final form 4 January 2024, accepted 26 February 2024)

ABSTRACT: Extreme wet-bulb temperatures (T_w) are often used as indicators of heat stress. However, humid heat extremes are fundamentally compound events, and a given T_w can be generated by various combinations of temperature and humidity. Differentiating between extreme humid heat driven by temperature versus humidity is essential to identifying these extremes' physical drivers and preparing for their distinct impacts. Here we explore the variety of combinations of temperature and humidity contributing to humid heat experienced across the globe. In addition to using traditional metrics, we derive a novel thermodynamic state variable named "stickiness." Analogous to the oceanographic variable "spice" (which quantifies the relative contributions of temperature and salinity to a given water density), stickiness quantifies the relative contributions of temperature and specific humidity to a given T_w. Consistent across metrics, we find that high magnitudes of T_w tend to occur in the presence of anomalously high moisture, with temperature anomalies of secondary importance. This widespread humidity dependence is consistent with the nonlinear relationship between temperature and specific humidity as prescribed by the Clausius–Clapeyron relationship. Nonetheless, there is a range of stickiness observed at moderate-to-high T_w thresholds. Stickiness allows a more objective evaluation of spatial and temporal variability in the temperature versus humidity dependence of humid heat than traditional variables. In regions with high temporal variability in stickiness, predictive skill for humid heat-related impacts may improve by considering fluctuations in atmospheric humidity in addition to dry-bulb temperature.

SIGNIFICANCE STATEMENT: Extreme humid heat increases the risk of heat stress through its influence over humans' ability to cool down by sweating. Understanding whether humid heat extremes are generated more due to elevated temperature or humidity is important for identifying factors that may increase local risk, preparing for associated impacts, and developing targeted adaptation measures. Here we explore combinations of temperature and humidity across the globe using traditional metrics and by deriving a new variable called "stickiness." We find that extreme humid heat at dangerous thresholds occurs primarily due to elevated humidity, but that stickiness allows for thorough analysis of the drivers of humid heat at lower thresholds, including identification of regions prone to low- or high-stickiness extremes.

KEYWORDS: Extreme events; Heat wave; Climate; Climate variability; Humidity

1. Introduction

Extreme humid heat events are climate extremes with important societal influence due to their direct link to human and animal heat stress. Physiological research has suggested that humid heat may pose additional risk to human health compared to dry heat due to humidity's influence over humans' thermoregulation efficiency (e.g., Mora et al. 2017; Parsons 2006; Steadman 1979; Fanger 1970). While increased dry-bulb temperatures alone can increase rates of dehydration, over 75% of the heat dissipation by human bodies is associated with evaporative cooling via sweating (Buzan and Huber 2020). The higher the ambient air specific humidity, the more difficult it is for sweat to cool our bodies by evaporation; at extremely high air temperatures, even a moderate amount of evaporative inhibition can cause heat stress. Exposure to this type of heat stress is widespread across the globe, and has been identified as one of the leading causes of death associated with climate extremes (Kovats and Hajat 2008).

Differentiating between extreme humid heat and extreme dry heat is essential to preparing for their individual impacts. At a given temperature, heat stress increases with elevated humidity, posing higher risk to human health and the potential

Denotes content that is immediately available upon publication as open access.

Supplemental information related to this paper is available at the Journals Online website: https://doi.org/10.1175/JAS-D-23-0072.s1.

Corresponding author: Catherine Ivanovich, cci2107@columbia.edu

Publisher's Note: This article was revised on 6 August 2024 to include the specific Github repository link in the Data Availability Statement for the code used in the study.

DOI: 10.1175/JAS-D-23-0072.1

for greater socioeconomic impacts than dry heat. In contrast, the presence of humidity may diminish the effect of extreme heat on crop growth by reducing vapor pressure deficit, for example, in the United States Midwest (Schauberger et al. 2017; Ting et al. 2023), and extreme dry heat has the potential to more strongly prime regions for wildfires (Abatzoglou and Williams 2016; Bowman et al. 2009).

The physical drivers of dry and humid heat extremes are also somewhat distinct. Extreme dry-bulb temperatures tend to occur due to blocking events associated with subsidence and clear sky conditions that lead to increased surface sensible heating (Röthlisberger and Papritz 2023; Photiadou et al. 2014), aridity that prevents the cooling effect of moisture evaporation (MacLeod et al. 2016), and urban heat island intensification (Horton et al. 2016; Tan et al. 2010). Raymond et al. 2021 suggests on the other hand that strong horizontal and vertical moisture fluxes, shallow boundary layers, nearby moisture sources such as warm water bodies, and stability that inhibits moist convection are key factors influencing extreme humid heat.

Due to these unique controlling mechanisms, the locations where the most intense dry and humid heat events tend to occur are also distinct. Extreme temperatures occur primarily in subtropical and lower-midlatitude deserts, while hotspots of humid heat have more geographic diversity (Rogers et al. 2021; Speizer et al. 2022). However, some locations do experience both types of extremes. An example is South Asia, which experiences intense dry heat extremes during the pre-monsoon season but where the increase in humidity associated with monsoon wind and rain can intensify local humid heat conditions (Raymond et al. 2020; Im et al. 2017; Ivanovich et al. 2024).

As a multivariate extreme composed of the co-occurrence of elevated humidity and temperature (Zscheischler et al. 2020), a given level of extreme humid heat can be generated by various combinations of temperature and specific humidity. Extremes that are driven largely by anomalous temperature or anomalous humidity have previously been described throughout the literature as temperature- or humidity-dependent, respectively (Raymond et al. 2017; Wang et al. 2019; Ivanovich et al. 2022). Distinguishing between these varieties of humid heat is especially important because while some adaptation measures, including increasing cities' tree and grass cover, effectively reduce local dry-bulb temperatures, the simultaneous increases in humidity they cause may weaken their benefits in addressing heat stress; furthermore, the efficacy of these adaptation strategies will themselves depend on the ambient combination of temperature and humidity (Chakraborty et al. 2022). Additionally, humid heat extremes of a given intensity created by high dry-bulb temperatures in the presence of some humidity have been shown in laboratory settings to be more detrimental to human health than those with moderate temperatures and very high humidity (Vecellio et al. 2022). This indicates that regions in which extreme humid and dry heat co-occur may also be the regions at highest risk for the most dangerous variety of heat stress.

Throughout the literature, the individual contributions from temperature and humidity toward a region's experience of humid heat are defined on a scale relative to typical local conditions (Raymond et al. 2017; Wang et al. 2019; Ivanovich et al. 2022). This has led to definitions of temperature and humidity dependence that are difficult to compare from one study to another. Given that substantial literature has developed on humid heat extremes, having a consistent and universal method for evaluating how these extremes are physically constituted from temperature and humidity is valuable for regional intercomparison, model evaluation, and further theoretical development, as well as for heat stress preparedness communication and adaptation.

To address this challenge, we first analyze the variability of humid heat conditions within a set of climatologically diverse case study regions using traditional metrics for temperature and humidity. We then derive a new thermodynamic state variable named "stickiness," apply it globally, and explore the additional insights it reveals. In section 2, we outline the methodologies used to evaluate the temperature and humidity dependence of extreme humid heat. Section 3 describes the results of these analyses. Section 4 reflects on the value, usability, and limitations of these different techniques, and provides suggestions for pathways forward.

2. Methods

a. *Variables of analysis*

We select wet-bulb temperature (T_w) as the primary humid heat variable for this analysis. It describes the lowest temperature a parcel of air could reach if it were cooled and moistened to the point of saturation by the adiabatic evaporation of liquid water at constant pressure (e.g., Bohren and Albrecht 1998). Thus, T_w is a thermodynamic state variable that provides a measurement of the efficiency of evaporative cooling, linking it directly to humans' experience of heat stress (Sherwood and Huber 2010). Particularly, T_w has been shown to exhibit thresholds beyond which survivability is limited, with the precise threshold value being dependent upon the physical characteristics of the individual experiencing the humid heat conditions (Vanos et al. 2023; Lu and Romps 2023; Vecellio et al. 2022). We calculate T_w using the Davies-Jones method (Davies-Jones 2008), which has been shown to more accurately capture extreme values than other calculation methods (Buzan et al. 2015).

We explore the global and regional relationships between T_w, dry-bulb temperature, and humidity using standard variables: specific humidity, relative humidity, and saturation deficit. To compute and analyze these variables, dry-bulb temperature, dewpoint temperature, and pressure data are retrieved from the HadISD station-based dataset (Dunn 2019). This dataset is produced by the Met Office Hadley Centre and records subdaily measurements from 8486 stations. We retrieve the full historical data record for each station, which is at most from year 1931 to year 2019 depending on individual station data availability. For each station, we calculate the daily maximum T_w at each station location and record the co-occurring temperature and specific humidity at this hour. We then use this data to calculate the co-occurring relative humidity and saturation deficit. We do not perform any preprocessing on the station data, relying on the Hadley Centre's quality control methods which include focus on the three variables

required to calculate T_w (temperature, dewpoint, and pressure) (Dunn et al. 2012). We note that the sampling frequency differences in a given year or between stations could influence the recorded trends in daily maximum T_w and that stations with lower sampling frequency are more likely to underestimate the magnitude of daily maximum T_w. We conclude that these challenges should not influence our results strongly as we do not compute trends and we are more interested in the co-occurring temperature and moisture at a range of T_w thresholds rather than the absolute magnitude of daily maximum T_w.

We then proceed to derive our new thermodynamic state variable—stickiness—quantifying the temperature and humidity dependence of a given value of humid heat.

b. *Thermodynamic state variable derivation*

1) PRIMARY DERIVATION METHODS—WET-BULB TEMPERATURE

After exploring information available from a wide range of diagnostics using traditional variables, next we create a novel method for quantifying the relative temperature and specific humidity dependence of humid heat by deriving a thermodynamic state variable analogous to oceanographic spice, which we refer to as "stickiness." Like spice, which represents how salinity and temperature jointly affect the density of water, stickiness captures the relative contributions of specific humidity and temperature to a given value of any variable which measures humid heat. Here, we focus on T_w as the target state variable, but the same approach can be applied to another metric of choice; we demonstrate this by extending the analysis to additional humid heat variables in following sections. By design, stickiness varies most with fluctuations in temperature and specific humidity at a given T_w, and least with changes in T_w itself.

Following the derivations for spice outlined by Flament (2002), we define a quantity whose variations in a temperature–specific humidity space are maximally distinct from those of T_w:

$$\frac{\partial_T \tau}{\partial_T T_w} + \frac{\partial_q \tau}{\partial_q T_w} = 0, \tag{1}$$

where T is temperature, q is specific humidity, T_w is wet-bulb temperature, and τ is stickiness, and $\partial_T \tau$ refers to $\partial \tau / \partial T$.

Stickiness is computed here as a polynomial equation, up to degree 3 in both temperature and specific humidity, constructed to satisfy Eq. (1) as described below. The T_w isopleths are close to linear in a temperature–specific humidity space, and degree three is thus sufficient to capture this structure (Fig. 4). Sensitivity to increasing the degree of the polynomial in each variable is negligible (not shown). The polynomial equation for stickiness can thus be expressed as

$$\tau(T, q) = -\sum_{i=0}^{3} \sum_{j=0}^{3} b_{ij} T^i q^j, \tag{2}$$

where b_{ij} refers to coefficients of term ij. This final derived polynomial equation allows for the calculation of stickiness given inputs of dry-bulb temperature and specific humidity.

We then compute the coefficients of the polynomial equation for stickiness numerically by performing a bound-constrained function minimization on an associated mean squared error. This mean squared error is defined as

$$\epsilon^2 = \lambda_1 \iint dT dq \left(\frac{\partial_T \tau}{\partial_T T_w} + \frac{\partial_q \tau}{\partial_q T_w} \right)^2 + \lambda_2 \iint dT dq \left(\frac{\partial_T \tau}{\partial_T T_w} - 1 \right)^2, \tag{3}$$

where the first and second terms represent the geometric and scaling constraints for stickiness, respectively, indicating that stickiness should be invariant for all geometric transforms and scaling changes allowed in the prescribed temperature–specific humidity domain. The second term also provides units with which to measure stickiness, determining here that stickiness has units of degrees Celsius. The λ_1, λ_2 are weights, set at 0.8 and 0.2, respectively. These derivation methods are relatively insensitive to changes in these weightings (not shown), and thus these values are selected following Flament (2002), to place greater dependence on the geometric constraint between the stickiness isopleths and the T_w isotherms over that of the scaling constraint. For more information, see Flament (2002).

The Nelder–Mead method using the Simplex algorithm is selected for the minimization (Nelder and Mead 1965; Wright 1996), with a tolerance for termination at 10^{-8} and a maximum of 100 000 function evaluations. This minimization search is executed on a temperature–specific humidity grid ranging from 25° to 50°C and 0 to 20 g kg^{-1} (with a resolution of 0.05°C and 0.04 g kg^{-1}), calculating T_w assuming a constant 1000 hPa surface pressure. Assuming a constant surface pressure reduces the dependence of stickiness upon pressure fluctuations in a given location. The elevations of global station locations used in this analysis range from −350 m (Ghor El Safi, Jordan) to 4736 m (T'u-Ko-Erh-Ho-Kung, China). However, the temperature–specific humidity space in which we conduct our derivation covers most of the tropics and midlatitude warm seasons, typically close to the 1000 hPa surface pressure selected. Further, we perform a sensitivity test in order to evaluate the effect of neglecting this pressure dependence and find that the resulting equation for stickiness is valid for surface pressures greater than 900 hPa (Fig. S1 in the online supplemental material), encompassing virtually all high-humid heat locations and events. Because extreme humid heat and its impacts attenuate rapidly with increasing elevation (decreasing pressure) (Raymond et al. 2022), we deem this to be a relatively minor caveat.

The derivation methods described are agnostic to the absolute magnitude and sign of stickiness. To aid in interpretability, the negative sign on the right hand side of Eq. (2) represents our chosen sign convention, where positive values of stickiness reflect higher humidity dependence. Further, the final equation for stickiness is shifted so that the zero value is equal to the mean conditions across all HadISD station locations (time averaging the full data record for each individual station and then taking the mean over all stations). Positive values of stickiness thus represent higher than average humidity

TABLE 1. Stickiness equation coefficients for T in °C and q in kg kg^{-1}.

Coefficients of term $T^i q^j$		j			
		0	1	2	3
i	0	−1.200	775.269	−7740.957	−7186.001
	1	−0.302	−3.086	238.012	−429.814
	2	−0.001 78	0.4987	−24.017	283.672
	3	0.000 027	−0.007 02	0.367	−5.094

dependence, while negative values represent higher than average temperature dependence. Unlike for dry-bulb temperature, a 0°C value of stickiness is unrelated to freezing. Due to the dominance of station density in Europe and North America, we perform a sensitivity test for this shift in the total magnitude of stickiness. We first average mean stickiness across 30° latitudinal bands (e.g., 0°–30°, 30°–60°, and 60°–90° in the Northern and Southern Hemispheres) and then take a weighted average across these six values based on the number of stations in each band (Fig. S2). This second method results in a global mean stickiness value just 0.6°C higher than the method using a simple mean. Given the mean standard deviation in stickiness during local summer across the globe is 1.3°C, the difference between these methodologies is relatively small and should not be expected to influence the presented results' interpretation.

Executing these derivation methods generates a polynomial equation for stickiness in terms of temperature and specific humidity, with the coefficients expressed in Table 1. Stickiness is measured in degrees Celsius due to the derivation's foundation on T_w, also with units of degrees Celsius. Worked examples highlighting the relationships between temperature, specific humidity, T_w, and stickiness are outlined in Table 2. We see, for example, that under annual mean conditions at a tropical location (here we select Jakarta, Indonesia for illustration), increasing the dry-bulb temperature by 1°C while holding specific humidity and pressure constant results in a decrease in stickiness of 2.2°C and an increase in T_w of 0.3°C. Under the same initial conditions, increasing specific humidity by 1 g kg^{-1} leads to an increase in stickiness of 0.6°C and an increase in T_w of 0.6°C.

The derivation methods described in this section can be applied to any humid heat metric that measures the combination of temperature and humidity, such as Humidex (Masterton and Richardson 1979) or moist static energy. The results of the derivation for Humidex are shown in Table S1 and Fig. S3. We have also applied these methods for moist static energy and compared our results to an analytic derivation in the following section. The code used for these numerical derivations is publicly available on Github for users interested in applying these methods to their humid heat metric of choice—the resulting units of stickiness may differ, but interpretation will be consistent.

2) SUPPLEMENTAL ANALYTICAL DERIVATION METHODS—MOIST STATIC ENERGY

While moist static energy (MSE) does not have the same direct link to heat stress as T_w and has not been explicitly related to the socioeconomic impacts of humid heat, these two variables are closely related to one another thermodynamically and should be expected to behave similarly. With this in mind, we also construct a version of stickiness based on MSE. Because it is analytically tractable, a derivation for stickiness based on MSE provides a simpler illustration of the concept than the numerical derivation method that is necessary for T_w. Moist static energy can be expressed as

$$\mathrm{MSE} = C_p T + gz + L_v q, \tag{4}$$

where C_p is the specific heat capacity, g is the gravitational constant, z is the vertical height, and L_v is the latent heat of

TABLE 2. Worked examples of tradeoffs between temperature, specific humidity, T_w, and stickiness. Initial conditions reflect a set of typical tropical conditions, here chosen as annual mean conditions at 1300 local time in Jakarta, Indonesia. Pressure (p) constant in all scenarios.

Initial conditions	Change applied	Resulting conditions
T = 28.4°C, q = 18.2 g kg^{-1}, p = 1009 hPa, stickiness = 2.9°C, T_w = 24.7°C	Holding q constant, increase temperature by 1°C to T = 29.4°C	stickiness = 0.7°C (−2.2°C), T_w = 25.0°C (+0.3°C)
	Holding T constant, increase specific humidity by 1 g kg^{-1} to q = 19.2 g kg^{-1}	stickiness = 3.5°C (+0.6°C), T_w = 25.3°C (+0.6°C)
	Holding stickiness constant, increase temperature by 1°C to T = 29.4°C	q = 18.6 g kg^{-1} (+0.4 g kg^{-1}), T_w = 25.2°C (+0.5°C)
	Holding stickiness constant, increase specific humidity by 1 g kg^{-1} to q = 19.2 g kg^{-1}	T = 30.8°C (+2.4°C), T_w = 25.9°C (+1.2°C)
	Holding T_w constant, increase temperature by 1°C to T = 29.4°C	q = 18.0 g kg^{-1} (−0.2 g kg^{-1}), stickiness = 2.3°C (−0.6°C)
	Holding T_w constant, increase specific humidity by 1 g kg^{-1} to q = 19.2 g kg^{-1}	T = 26.4°C (–2.0°C), stickiness = 4.0°C (+1.1°C)

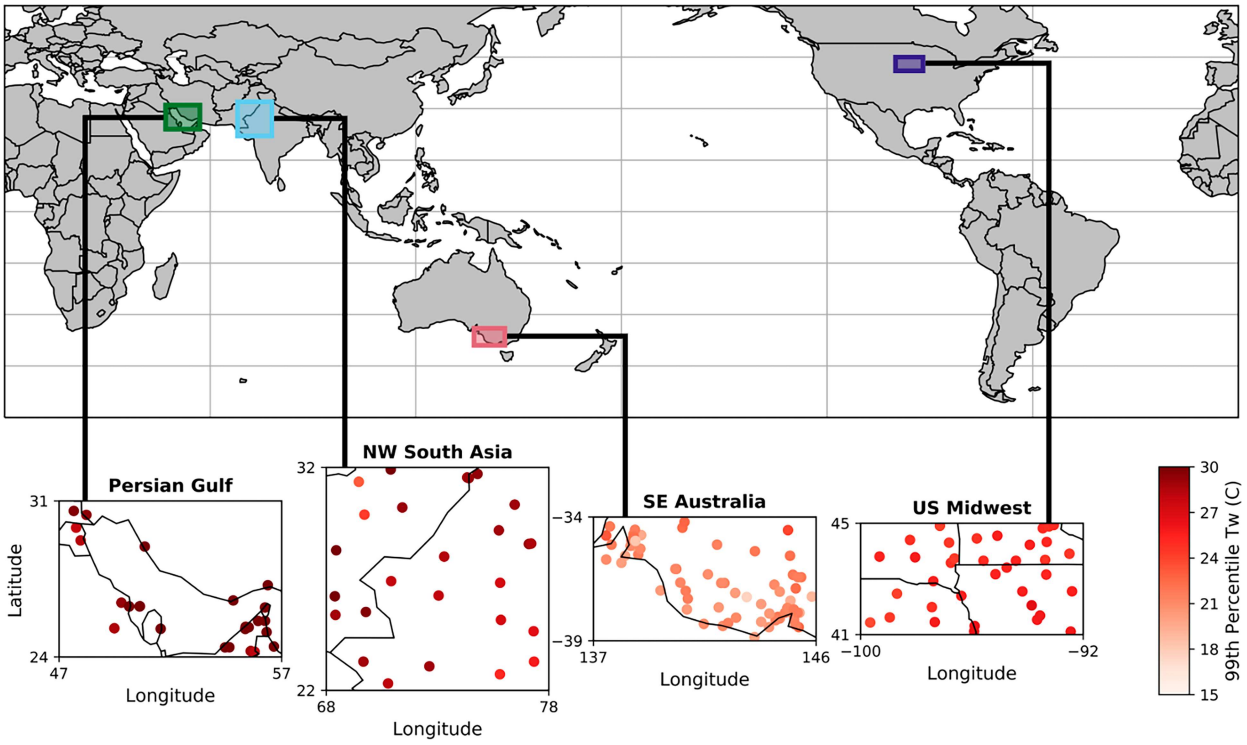

FIG. 1. HadISD station locations included in regional analyses, colored by 99th-percentile daily maximum T_w (full year). Four boxed regions of interest are referred to as Persian Gulf, NW South Asia, SE Australia, and U.S. Midwest.

vaporization. At the surface ($z = 0$), this expression simplifies to a linear combination of temperature and specific humidity:

$$\mathrm{MSE} = C_p T + L_v q. \tag{5}$$

In this case, deriving stickiness as a variable whose changes in temperature–specific humidity space are maximally distinct from those of our humid heat variable—now surface MSE—can be executed analytically, yielding the result:

$$\tau_{\mathrm{MSE}} = C_p T - L_v q \tag{6}$$

or

$$\tau_{\mathrm{MSE}} = -C_p T + L_v q, \tag{7}$$

where Eq. (7) has been assigned the same sign convention described in the numerical derivation above for T_w, with high (low) stickiness reflecting humidity-dependence (temperature-dependence).

We use this MSE-based derivation in order to help clarify the goal of our numerical derivation, as well as to check its accuracy against the analytical solution. Indeed, the solutions are in close agreement (Fig. S4). We present a second set of results for the MSE-based derivation in the supplement, but focus on the T_w-based definition in the main text due to our motivation to capture patterns relevant to societal impacts. We find similar overall conclusions from each derivation method (Figs. S18 and S19).

c. *Regional comparisons*

We explore the relationships between temperature, humidity, and humid heat by comparing patterns in existing heat and humidity variables identified in four climatologically distinct regions. These regions are the Persian Gulf (20°–36°N, 45°–60°E, restricted to stations with a 99th-percentile T_w above 28°C), northwestern South Asia (22°–32°N, 68°–78°E,), southeastern Australia (28°–39°S, 141°–154°E,), and the U.S. Midwest (41°–45°N, 92°–100°W,) (Fig. 1). The first two regions (Persian Gulf and NW South Asia) were selected based on their historical propensities for extreme humid heat (Raymond et al. 2021; Rogers et al. 2021; Raymond et al. 2020). In both of these locations, extreme humid heat events depend strongly on moisture modulation yet are associated with unique large-scale meteorological patterns across distinct geographies (Pal and Eltahir 2016; Im et al. 2017; Monteiro and Caballero 2019; Mishra et al. 2020; Ivanovich et al. 2022, 2024). Southeastern Australia (hereafter, SE Australia) was selected to provide contrast to these humid heat hotspots, due to its Mediterranean climate with lower summer humidity. The U.S. Midwest was selected due to the complex influence of cropland on humid heat in the area, shown to increase local humidity but decrease local dry-bulb temperatures (Coffel et al. 2022; Ting et al. 2023; Mueller et al. 2016). We note that all regional analyses in this study treat daily-scale station measurements as individual data points, rather than averaging conditions across stations. The aggregation of these stations may complicate interpretation due to the potential grouping

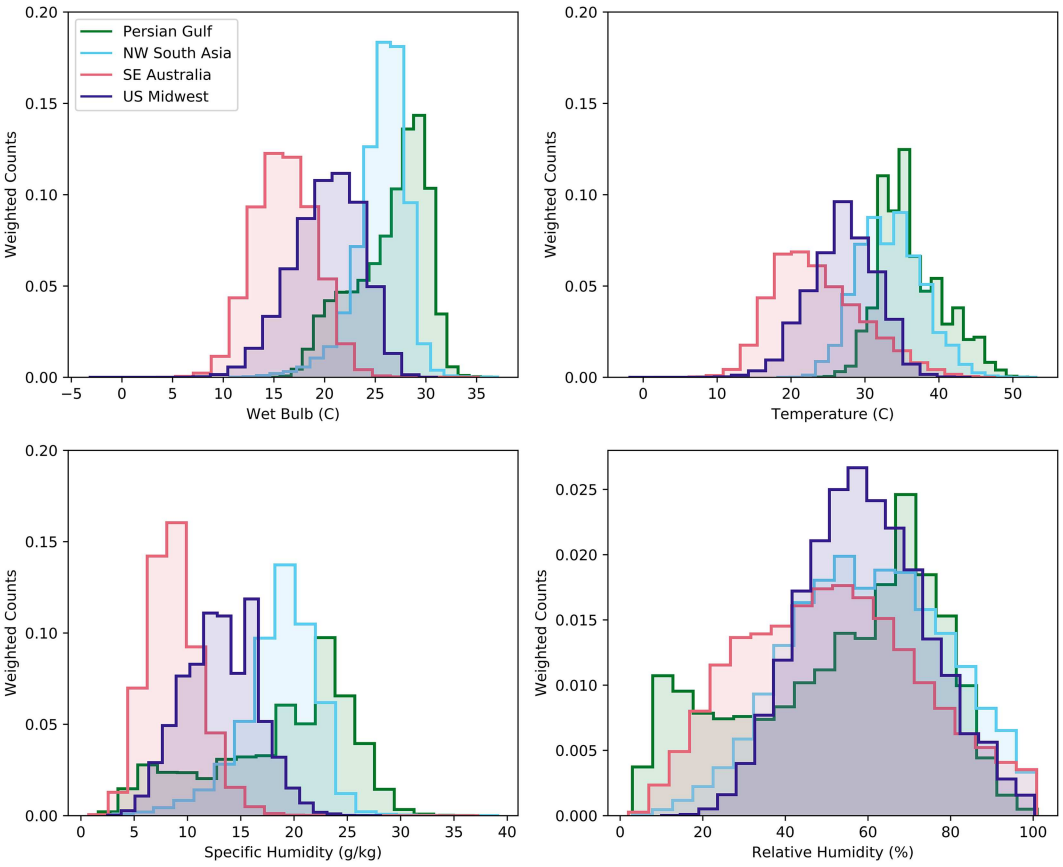

FIG. 2. Histograms of (top left) T_w, (top right) dry-bulb temperature, (bottom left) specific humidity, and (bottom right) relative humidity in the four regions of interest. Shown for local summer season (JJA for the Persian Gulf, NW South Asia, and the U.S. Midwest; DJF for SE Australia). Note the smaller y-axis range in the bottom-right panel to visualize shape of the broader distributions.

of diverse locations into the boxed boundaries described above. Such limitations motivated the additional selection criterion for the Persian Gulf region in order to avoid dry, mountainous locations in Iran which experience drastically different climatologies than the rest of the stations in the region. Single station scale analyses were also performed when necessary to help discern the source of variability in identified patterns.

3. Results

a. *Exploration of temperature and humidity combinations through traditional variables*

Our four case study regions experience varying intensities of humid heat and distinct mechanisms which bring about local humid heat extremes. First, these regions exhibit contrasting distributions in temperature, humidity, and T_w (Fig. 2). Each of the four regions has a unimodal temperature distribution. This is also true for T_w, specific humidity, and relative humidity in all regions except for the Persian Gulf, which has a bimodal distribution in these three variables. The areas surrounding the Persian Gulf are very dry throughout the Northern Hemisphere summer, but the advection of marine air through strong sea breezes and synoptic scale meteorological conditions increases local humidity and under certain conditions can drive T_w into dangerous thresholds (Ivanovich et al. 2022; Raymond et al. 2021; Pal and Eltahir 2016; Xue and Eltahir 2015). We note that removing the requirement that all stations in the Persian Gulf region exhibit a 99th-percentile T_w above 28°C increases the spread of these distributions in specific humidity, relative humidity, and T_w (not shown), but that the bimodal distributions is retained for all thresholds tested between 25° and 30°C. Further, this bimodality is consistent across the individual station locations selected for this region, and an example using a station in Dammam, Saudi Arabia, is plotted in Fig. S5 for reference.

To visualize the full record of daily-scale station data within each region, we plot the dry and wet-bulb temperature at the hour of recorded daily maximum T_w against a variety of co-occurring humidity metrics: specific humidity, relative humidity, and saturation deficit. We find that locally extreme dry-bulb temperatures can occur at a range of specific humidities, although consistently low relative humidities (Figs. 3a,c). In NW South Asia, elevated temperatures are associated with changes in specific humidity which in combination generate a

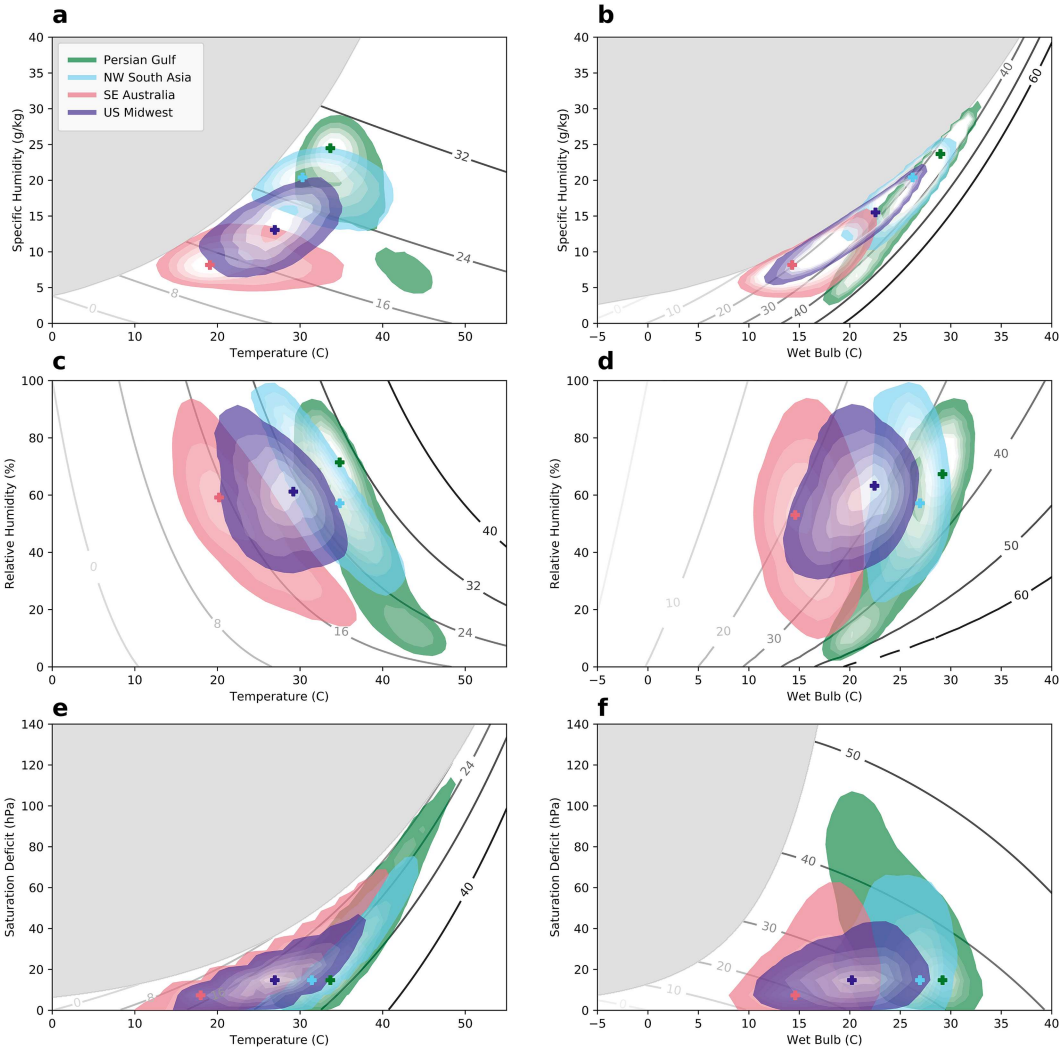

FIG. 3. Daily temperature and humidity conditions for the historical data record over all stations in each region. (left) Temperature and (right) T_w compared to (a),(b) specific humidity, (c),(d) relative humidity, and (e),(f) saturation deficit. Shaded contours indicate Gaussian kernel density estimation of conditions during daily maximum T_w for each region (with colored crosses at the distributions' centers); gray contours indicate (left) T_w and (right) dry-bulb temperature isotherms. Gray shading indicates conditions producing supersaturated air. Shown for local summer season (JJA for the Persian Gulf, NW South Asia, and the U.S. Midwest; DJF for SE Australia).

relatively small range in T_w compared to the other three regions. This indicates a tendency for compensatory effects, whereby temperatures vary more than specific humidity and variations in specific humidity tend to partially offset those in temperature, possibly indicative of the simultaneous cooling and moistening effect of evaporation of soil moisture or surface water. In the U.S. Midwest, high temperatures are associated with high specific humidities, suggesting a larger potential for elevated temperature and specific humidity to co-occur, with both factors contributing to extreme T_w. The most extreme T_w days in SE Australia occur at moderately high temperatures (roughly 35°C) when the air is virtually saturated (Fig. S6). A bimodal distribution is again evident in the Persian Gulf, with the majority of days at high temperatures and high specific humidities, which contrasts with a smaller cluster of extreme temperature dry days. In all four regions, the highest recorded T_w are associated with the highest recorded specific humidity conditions (Fig. 3b). Further, the distribution of conditions in each region shows that increases from locally moderate to extreme T_w cross few temperature isotherms, suggesting that extreme humid heat conditions tend to be humidity dependent.

We also observe that the most extreme temperatures are associated with a small range of very low relative humidities in three of the regions. The relative humidities that occur with extreme T_w apparently differ more widely than those that occur with extreme temperatures. In the Persian Gulf, NW South Asia, and SE Australia, increasing temperatures are closely associated with decreasing relative humidities, hewing fairly closely to lines of constant T_w (Fig. 3c). At locally high T_w thresholds, the distributions in NW South Asia and SE

Australia cross many temperature isotherms (Fig. 3d), indicating that extreme temperatures are not a necessary component to generating humid heat extremes in these regions. The associated relative humidities also vary substantially, though still within the upper half of the local distribution (Fig. 3d). The bimodal structures in the relationships between relative humidity and both temperature and T_w are again clear in the Persian Gulf, delineating between days that are hotter and drier versus cooler and moister. NW South Asia experiences most summer days in a high relative humidity environment, while the relative humidity and T_w conditions in the U.S. Midwest are lower and more consistent than the other three regions.

While extreme T_w can exhibit a slightly larger range in saturation deficit than extreme dry-bulb temperatures, this difference is not as pronounced as for relative humidity. The highest recorded temperatures in each region are associated with the highest recorded saturation deficits (Fig. 3e). Further, changes in temperature are compensated by changes in saturation deficit which keep T_w at a roughly constant intensity. Extreme T_w in the Persian Gulf, SE Australia, and the U.S. Midwest are limited to those days very close to saturation (Fig. 3f). In NW South Asia, in contrast, extreme T_w span a range of saturation deficits and cross many dry-bulb temperature contours. The T_w in the U.S. Midwest and SE Australia tend to be lower with small ranges in saturation deficits, suggesting both that temperature and specific humidity tend to fluctuate jointly in these regions, and that an absence of very high temperatures may limit how large saturation deficits can be. In each panel of Fig. 3, the strong relationship between certain heat and humidity metrics is evident. Particularly, relative humidity and saturation deficit depend strongly on temperature, which is reflected in the same correlation sign between these variables in the four case study regions. Conversely, while retaining some dependence on temperature, T_w is much more sensitive to specific humidity than to the other two humidity variables, sharing a consistent increase with specific humidity that is not observed with relative humidity or saturation deficit.

Overall, we conclude that while high dry-bulb temperatures can occur at a range of moisture levels, the occurrence of extreme humid heat is much more limited to a narrow range of anomalous humidity (most clearly when measured by specific humidity). However, there are a small fraction of days associated with highly elevated dry-bulb temperatures in the presence of moderate humidity that together causes extreme T_w. The various combinations of these standard variables, in multiple plots made from long-term station records in each region, allows us to draw these conclusions with some confidence and nuance. However, extending this analysis to a global scale by recreating these plots for all station locations would be intractable. The lack of a global benchmark for meaningfully comparing disparate temperature and humidity combinations adds another complication. We could thus hope for a more direct route to these conclusions, and especially one that allows us to compare the humidity or temperature dependence of humid heat in locations around the world more straightforwardly and objectively. Toward this end, we use the following section to explore the use of stickiness, whose derivation was outlined above.

b. *Stickiness derivation results and analysis*

Above we derived a thermodynamic state variable, stickiness, which varies most with fluctuations in dry-bulb temperature and specific humidity and is least correlated with T_w. Our methods generate a consistent and globally applicable scale with which to compare the temperature versus specific humidity contributions toward a given intensity of T_w.

While the derivation above constrains the units of stickiness to be degrees Celsius, the location of the intercept (0°C) is arbitrary and constructed here so that the mean value over all stations' historical records is 0°C. With this choice, we also observe that a large fraction of conditions observed on Earth occur around 0°C (Fig. 4). The mean conditions in the four case study regions are also close to this zero value, while their 99th-percentile T_w conditions are all at positive stickiness. This supports the conclusion reached by previously published literature that extreme humid heat tends to be humidity dependent (e.g., Raymond et al. 2020; Lutsko 2021). This pattern is also supported by our physical understanding of the relationship between temperature and specific humidity. Due to the Clausius–Clapeyron relationship, higher dry-bulb temperatures are associated with the ability for air to experience exponentially higher specific humidity before reaching saturation. This allows the potential magnitude of local specific humidity variations to increase nonlinearly with temperature, suggesting that the contributions of humidity fluctuations to extreme humid heat may be greater than those of dry-bulb temperature fluctuations. Similarly, it implies certain seasonal and geographic patterns of stickiness as explored in later sections. As the climate continues to warm, higher latitudes will likely see greater variability in specific humidity along with that in temperature (Lutsko 2021) and occasional high-stickiness conditions may progress further poleward. Additionally, comparing the stickiness contours in Fig. 4 with the relative humidity and saturation deficit contours in Fig. 3, stickiness does not exhibit the same nonlinearities at extreme temperatures. Stickiness may thus be a useful diagnostic at very high and low temperatures.

Stickiness is a single variable that measures the spatial variability of global humid heat temperature versus humidity dependence. During the hour of recorded daily maximum T_w for all days in each station record, high stickiness is found commonly in coastal regions (Figs. 5a and 6a). Regions with monsoon climates also exhibit higher stickiness in rainy seasons than in dry seasons. For example, South Asia tends to experience higher stickiness during the June–August (JJA) season than the December–February (DJF) season. The lowest values of stickiness under both mean and extreme conditions are at high elevation, including the regions near the Andes Mountains, the Tibetan Plateau, and the Rocky Mountains. Summer patterns in stickiness for the Northern and Southern Hemispheres (when local T_w are more intense) are distinct. Namely, mean stickiness conditions in the Southern Hemisphere are not nearly as high as those in the Northern

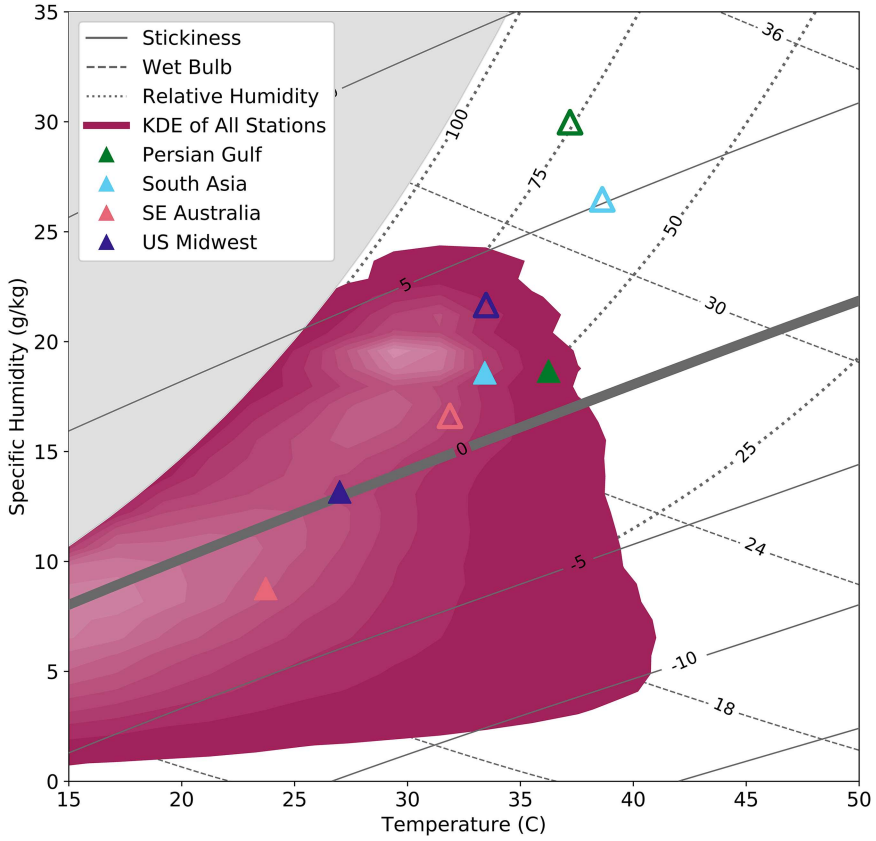

FIG. 4. Families of T_w isotherms and stickiness isopleths. Zero value calculated based on mean stickiness conditions associated with all station locations (full-year data), as shown by the magenta shading. Gray shading indicates supersaturated conditions. Filled (open) triangles indicate regional mean stickiness conditions on all days in the year (99th-percentile T_w days). Dotted gray lines indicate relative humidity isopleths.

Hemisphere, consistent with the observation that there is higher mean specific humidity in the Northern Hemisphere compared to the Southern Hemisphere (Dai 2006). Further, high stickiness under mean T_w extends to much higher latitudes on the eastern coast of North America and Asia during JJA than do those in the Southern Hemisphere during DJF (Figs. 5a and 6a), but these stickiness values decrease rapidly toward the west into the interior of each continent. Additionally, a higher fraction of tropical Northern Hemisphere stations exhibit positive stickiness under mean conditions during DJF than do tropical Southern Hemisphere stations during JJA. The highest temporal standard deviation in stickiness tends to occur in semiarid coastal regions (Figs. S14a and S15a). These include southeastern Australia, South Africa, and the Sahel, each of which experiences large interannual climate variability including strong influences of the El Niño–Southern Oscillation (ENSO) phenomenon. Stickiness also exhibits high variability in extreme humid heat hotspots, where the mean values are also large.

Stickiness is higher during extreme T_w events than during mean conditions at most stations around the globe during the local summer season. In fact, many stations have never reached a locally extreme T_w under low-stickiness conditions, and this is particularly true in regions where the 99th-percentile T_w threshold is sufficiently high to impact human health, such as the Persian Gulf, South Asia, the Sahel, and the Amazon basin (Fig. S16). Around the globe, stickiness is constrained to positive values during high intensity humid heat days, while there is a larger range of stickiness during more moderate humid heat conditions (Fig. S17). At the same time, some regions do maintain their overall temperature dependence (low stickiness) even on locally extreme T_w days. These stations include those located in the western United States, the Sahara, Iran, and Chile and are primarily in continental-interior locations which have no pathway for advection of warm and humid air from a surrounding water body or region of high soil moisture. However, for a subset of near-coastal stations—for example, in Alaska and on the Scandinavian coast—the low stickiness may be a consequence of the cool sea surface temperatures offshore, and could change as those temperatures warm. While nearly all stations exhibit an increase in stickiness on extreme T_w days in the JJA season, there are some decreases in stickiness on extreme T_w days in the Northern Hemisphere during DJF, when T_w is relatively low. We note that there is not an equivalently large landmass below 40°S harboring cold, dry air (such as northern North America or

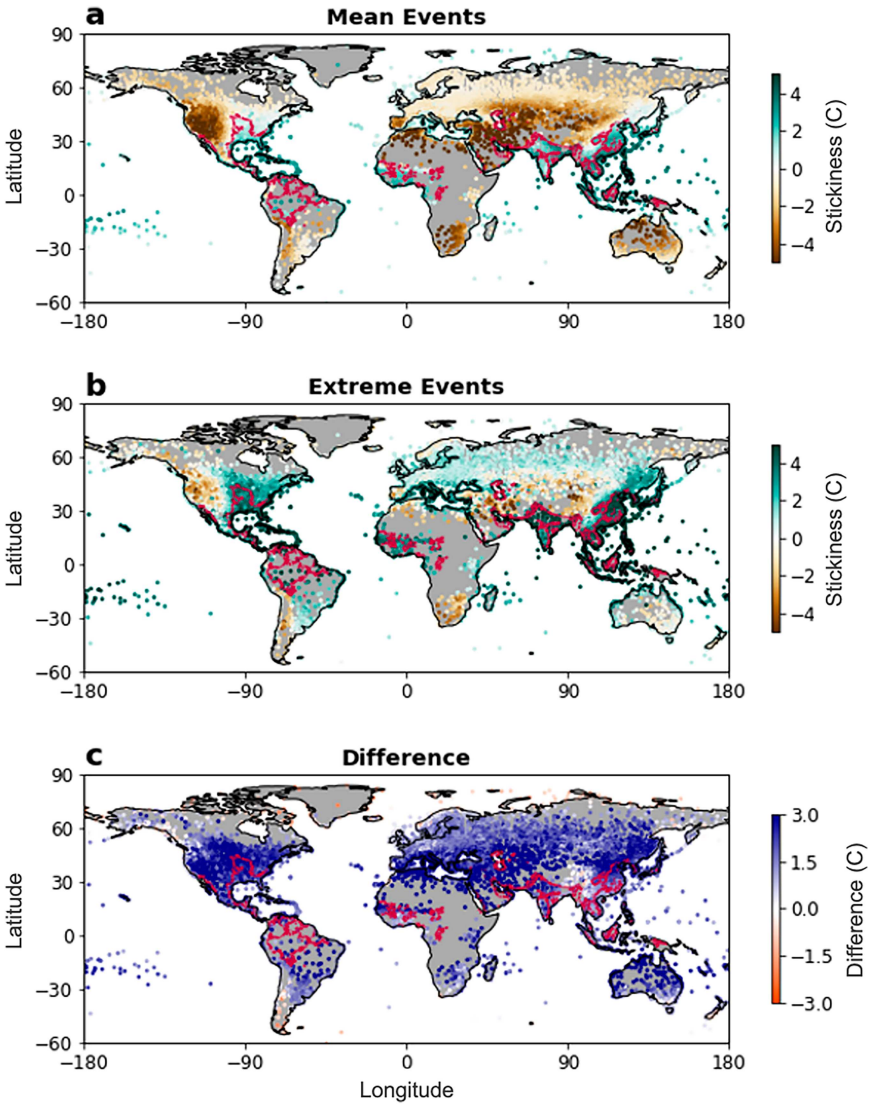

FIG. 5. Global maps of mean stickiness during the hour of daily maximum T_w at each station location based on subset of the data record during JJA season: (a) data from all days in each station record, (b) data from 99th-percentile T_w days, and (c) difference between these two maps in (b) and (a). Red contours indicate regions with 99th-percentile T_w above 27°C (based on JJA season, ERA5 gridded data; Hersbach et al. 2020).

Eurasia) that could compare for the Southern Hemisphere in JJA. Spatial patterns in the standard deviation of stickiness are similar for extreme T_w conditions as under mean conditions in both seasons, but the magnitude is generally lower during extreme events (Figs. S14b and S15b).

The patterns described above are not directly observable by plotting the global dry-bulb temperature, specific humidity, or relative humidity associated with mean and extreme humid heat events (Figs. 7 and 8). All stations show both higher specific humidity and dry-bulb temperature on extreme humid heat days than during average humid heat conditions, regardless of season. Some regions do exhibit decreases in local relative humidity on these extreme humid heat days, such as Alaska, northern Europe, and southeast China. However, these three locations all experience increases in stickiness during extreme humid heat days compared to mean conditions (Fig. S20). These extreme days associated with decreased relative humidity but increased stickiness may result from the disparity between the exponential increase in saturation vapor pressure and the linear increase in stickiness associated with elevated temperatures (Fig. 4). Such events could be caused by flow from the continents' dry interior or strong transient high pressure systems that could increase local dry-bulb temperatures without concomitantly increasing moisture sufficiently to maintain relative humidity (Zscheischler and Seneviratne 2017). In contrast, during DJF seasonally high-

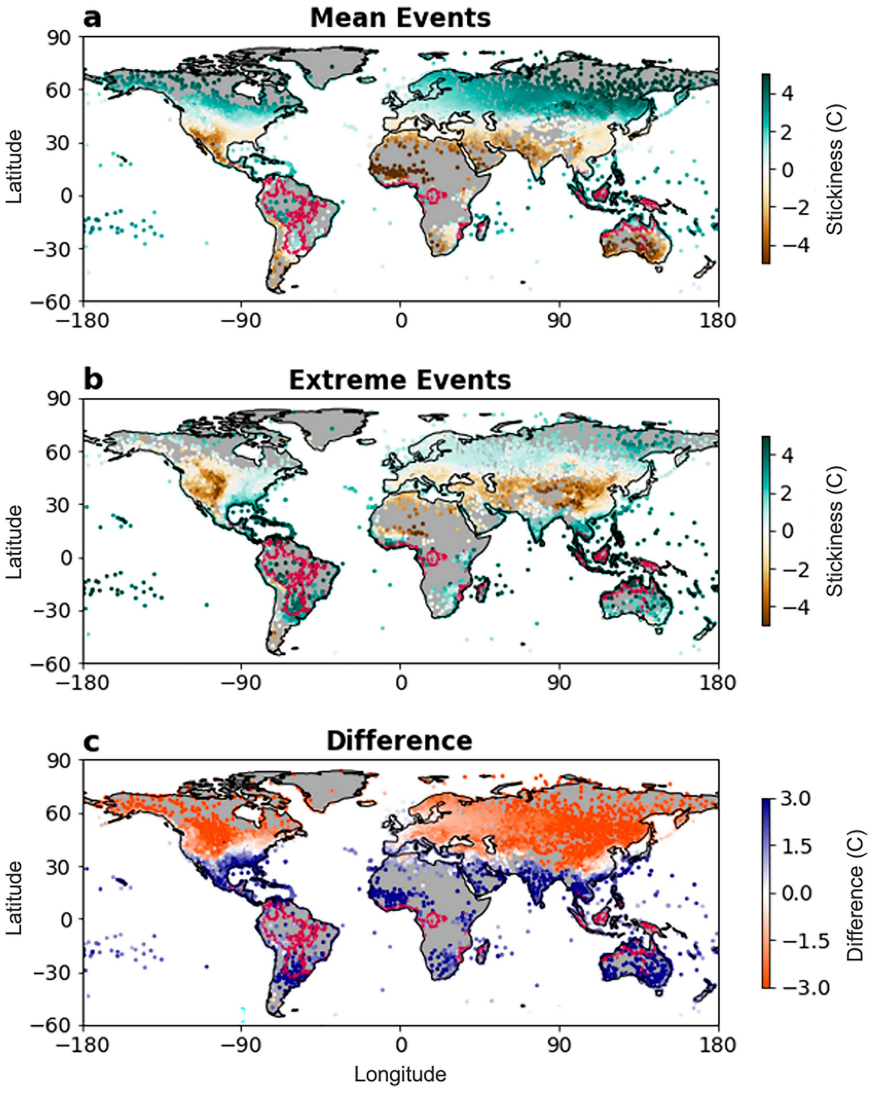

FIG. 6. Global maps of mean stickiness during the hour of daily maximum T_w at each station location based on subset of the data record during DJF season: (a) data from all days in each station record, (b) data from 99th-percentile T_w days, and (c) difference between these two maps in (b) and (a). Red contours indicate regions with 99th-percentile T_w above 27°C (based on DJF season, ERA5 gridded data).

humid heat events, regions such as the western United States, central Europe, Eurasia, and eastern China exhibit decreases in relative humidity while experiencing strong decreases in stickiness. The seasonal differences in the relationship between relative humidity and stickiness reflect the distinct seasonal climatologies in the Northern Hemisphere, as baseline dry-bulb temperatures are much higher in the summer than the winter.

The spatial patterns in the difference in stickiness during mean versus extreme humid heat days are most similar to those of specific humidity, with the largest differences in regions such as the Persian Gulf and the Gulf of California in JJA and the southeastern United States, the Sahel, and Australia in DJF (Figs. 7a and 8a). This similarity in spatial patterns between stickiness and specific humidity is again consistent with the Clausius–Clapeyron relationship. The nonlinear relationship between temperature and specific humidity suggests that at moderate-to-high temperatures, specific humidity fluctuations may be more critical than dry-bulb temperature fluctuations to the achievement of extreme T_w values. Spatial patterns in specific humidity changes have thus been shown to drive those of humid heat (Lutsko 2021), which is reflected in global stickiness patterns. The key difference in the spatial pattern of these two variables is that while all stations exhibit higher specific humidity during extreme T_w days than during average conditions, this is not the case for stickiness (particularly in high northern latitudes during boreal winter). The magnitude of

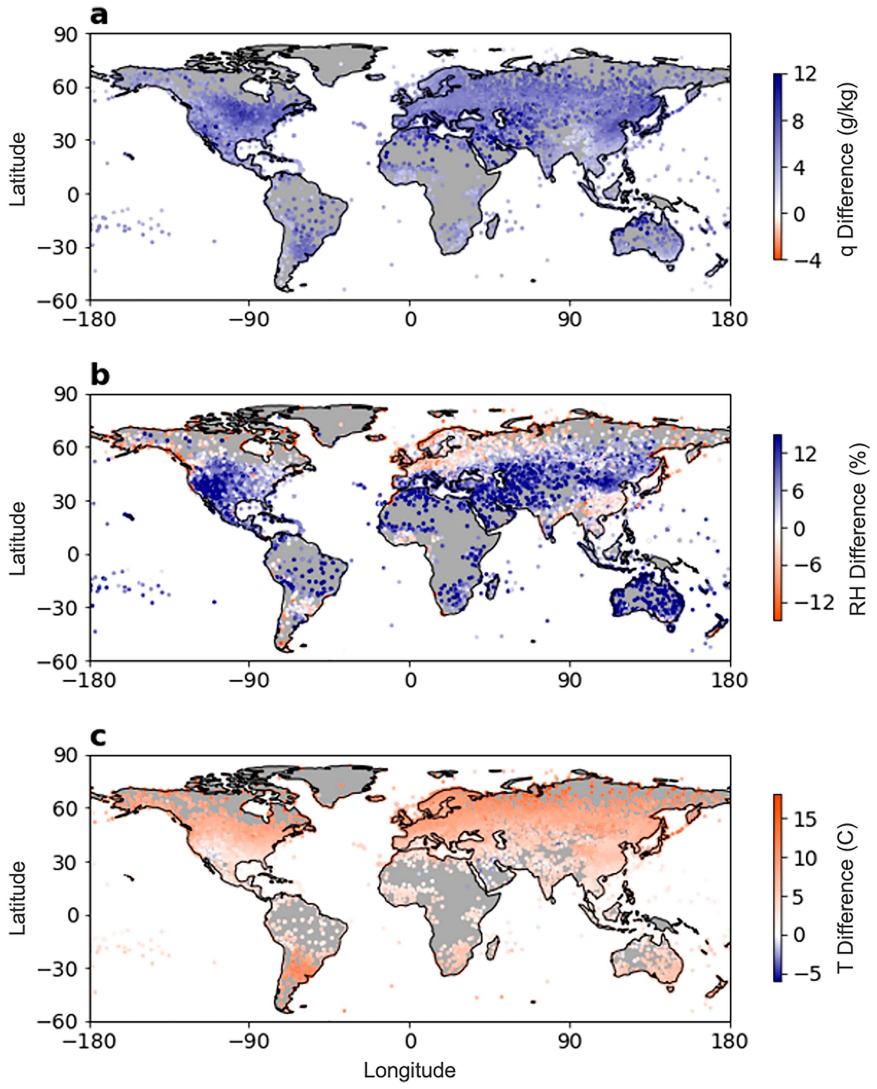

FIG. 7. Global maps of mean (a) specific humidity, (b) relative humidity, and (c) temperature during hour of daily maximum T_w at each station location based on subset of the data record during JJA season. Each plot shows the difference between the conditions occurring during extreme T_w days compared to all days (analogous to Fig. 5c).

specific humidity increases are comparable across much of each summer hemisphere, and can even increase with latitude in regions such as the United States in JJA and Australia in DJF, indicating the large intraseasonal variability at these latitudes.

Returning to the four case study regions and exploring the temporal variations in the relationships between stickiness and humid heat further highlights the dependency of extreme T_w on anomalous specific humidity (high stickiness). In each region, the highest recorded T_w occur at the highest stickiness values, following along the saturation curve (Fig. 9). However, there is a large range in stickiness at locally defined moderate levels of humid heat, particularly in the Persian Gulf and NW South Asia. At a threshold of 27°C, these two regions experience a range of stickiness from about −1° to 5°C. The larger range in stickiness associated with moderately high T_w thresholds within these two individual regions is consistent with the increased spatial variability in global stickiness at moderately high T_w intensities (Fig. 10). We note that 4640 HadISD stations have experienced T_w thresholds between 25° and 26°C in their historical records, with a range of both negative and positive co-occurring stickiness conditions. In contrast, only 1982 stations have previously recorded T_w conditions between 29° and 30°C, and the co-occurring stickiness is consistently higher, with an average stickiness across stations of 5.2°C. In SE Australia and the U.S. Midwest, low T_w conditions are associated with relatively low dry-bulb temperatures and increased stickiness. In these midlatitude (rather than subtropical) regions, jet stream variability may influence local temperature and moisture conditions and drive these patterns (He et al. 2023). It is also

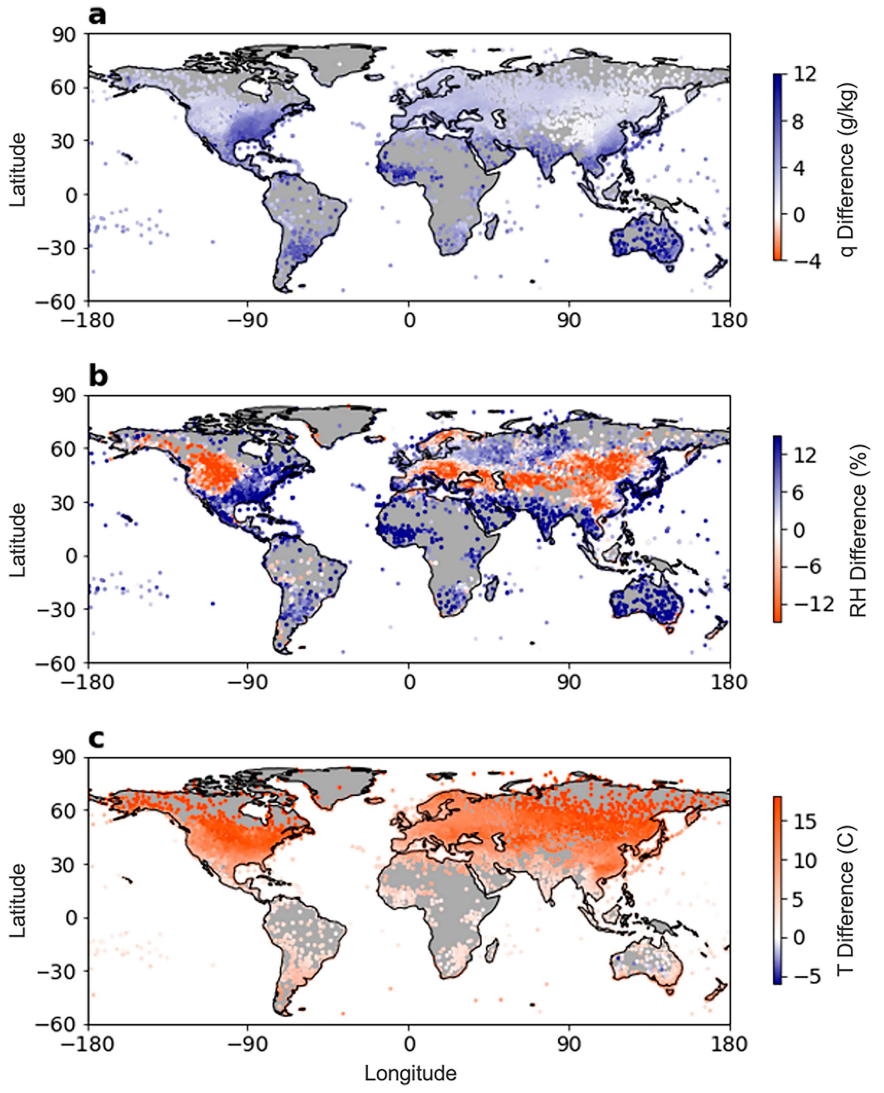

FIG. 8. Global maps of mean (a) specific humidity, (b) relative humidity, and (c) temperature during hour of daily maximum T_w at each station location based on subset of the data record during DJF season. Each plot shows the difference between the conditions occurring during extreme T_w days compared to all days (analogous to Fig. 6c).

possible that vegetation cover within these regions helps supply moisture during the summer months, preventing severely low specific humidity levels even as dry-bulb temperatures drop. The distinct summers of 2011 and 2012 in the U.S. Midwest are examples illustrating the range of stickiness at moderate T_w thresholds in this region. The hot and dry summer of 2012 was widely reported on due to the experience of flash droughts (e.g., Mallya et al. 2013; Otkin et al. 2016). While the preceding summer only experienced moderate dry-bulb temperatures, observed T_w values throughout the region were actually higher than in 2012 (Fig. S21). Stickiness can help to characterize the contrasting conditions that dominated these summers—both in the bulk of the distribution and in the tails, as well as distinguishing primarily temperature-driven versus primarily humidity-driven differences—without resorting to combinations of other temperature and humidity variables.

As discussed in the introduction, existing approaches to quantifying the temperature and humidity contributions to T_w extremes tend to be defined on scales that are specific to a given location and depend on the typical ranges in these variables that occur there. Stickiness aims to be more broadly relevant and allow greater ease of comparison between climates. Stickiness is arguably still most valuable in a relative sense, however, in that its variations are systematically different at different T_w values as shown above. In particular, very high T_w tends to only occur concurrently with high stickiness, while stickiness varies more widely at lower T_w. Stickiness provides the greatest insights into the physical drivers of extreme humid heat when evaluating it at similar T_w values (i.e., along a

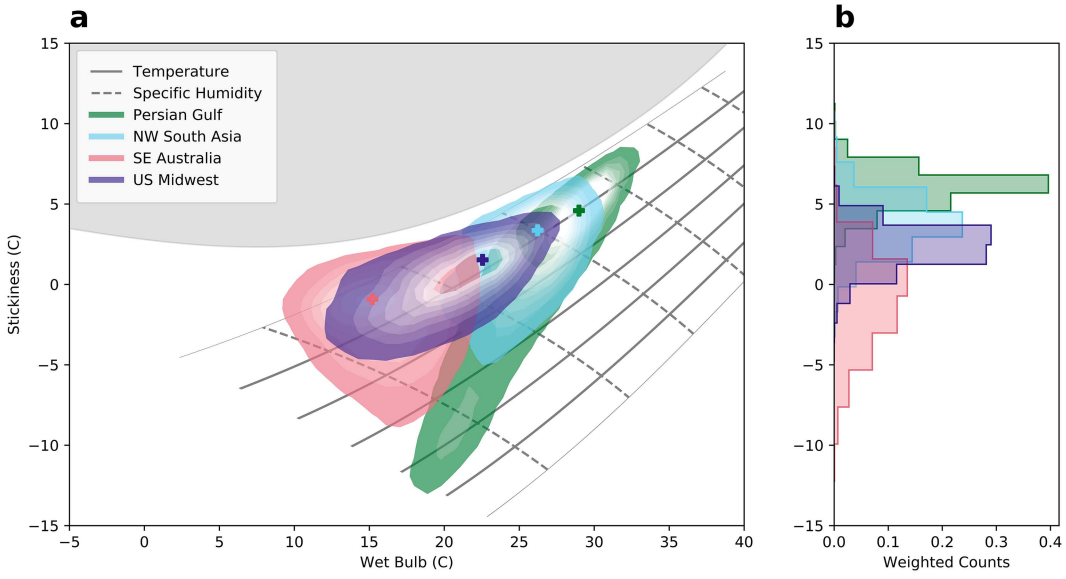

FIG. 9. (a) Daily T_w and stickiness occurring at the hour of daily maximum T_w for historical data record over all stations in each region. Shaded contours indicate Gaussian kernel density estimations; gray solid (dashed) contours indicate temperature (specific humidity) isopleths. Gray shading indicates conditions producing supersaturated air. Shown for local summer season (JJA for the Persian Gulf, NW South Asia, and the U.S. Midwest; DJF for SE Australia). (b) Stickiness distributions during 90th-percentile T_w days in each region.

vertical line in Fig. 9). Comparisons across very different regions and seasons reveal stickiness' inherent sensitivity to baseline temperature, since the Clausius–Clapeyron relationship dictates that the latent heat of a parcel increases faster than its dry enthalpy with temperature. This also implies that in general under climate change, latent heat will contribute ever more to the total moist static energy and related T_w (Matthews 2018; Lutsko 2021), increasing the fraction of global extreme events with high stickiness.

However, in contrast to existing approaches, the utility of stickiness as a diagnostic is not relative in the sense of depending on the range of variability within a given climate. It need only be defined once, rather than many times for different locations, and comparing two stickiness values occurring at the same T_w is meaningful even if the two observations were taken from different locations with different ranges of seasonal or subseasonal variation. We conclude that, while no single diagnostic meets all possible needs, stickiness may be a useful addition to existing variables for analyses of the contributions of temperature and humidity to variations in T_w or other measures of humid heat.

4. Discussion and conclusions

While the relative dependence of humid heat on temperature and humidity varies spatially and temporally across the globe, we find that extreme humid heat at thresholds sufficiently high to impact human health tends to be humidity-dependent—that is, associated with relatively large moisture anomalies rather than temperature anomalies. We have demonstrated this phenomenon by examining the historical record of traditional metrics such as dry-bulb temperature, specific humidity, relative humidity, and saturation deficit within a set of climatologically diverse case study regions. We also show that variation in this dependence can be succinctly described using the newly derived variable stickiness, which allows for the direct comparison of the varying dependencies of humid heat, both within one location across time and at one time across the globe.

The global consistency of stickiness allows for the comparison of the potentially unique regional dynamics leading to local humid heat extremes. We find that the difference in stickiness between mean and extreme humid heat days has some common features across the globe, homogeneous at local scales and heterogeneous at regional scales. Humid heat at high magnitudes tends to be humidity-dependent (high stickiness). This is consistent with recent literature investigating the dynamics of extreme events in humid heat hotspots, highlighting key factors and processes such as moisture advection (Monteiro and Caballero 2019; Ivanovich et al. 2024) and proximity to warm water bodies or irrigated land (Im et al. 2017; Mishra et al. 2020; Krakauer et al. 2020; Jha et al. 2022). The importance of such processes underscores the influence of moisture modulation for driving humid heat extremes, especially when paired with stability against deep convection (Raymond et al. 2021). We also find that regions at high elevation including the areas "downwind" of mountain ranges all exhibit low-stickiness conditions during both mean and extreme humid heat days. While it is difficult for T_w at high elevation to exceed dangerous thresholds for human health (Raymond et al. 2022), these results highlight that the fluctuations in temperature in these relatively dry environments are

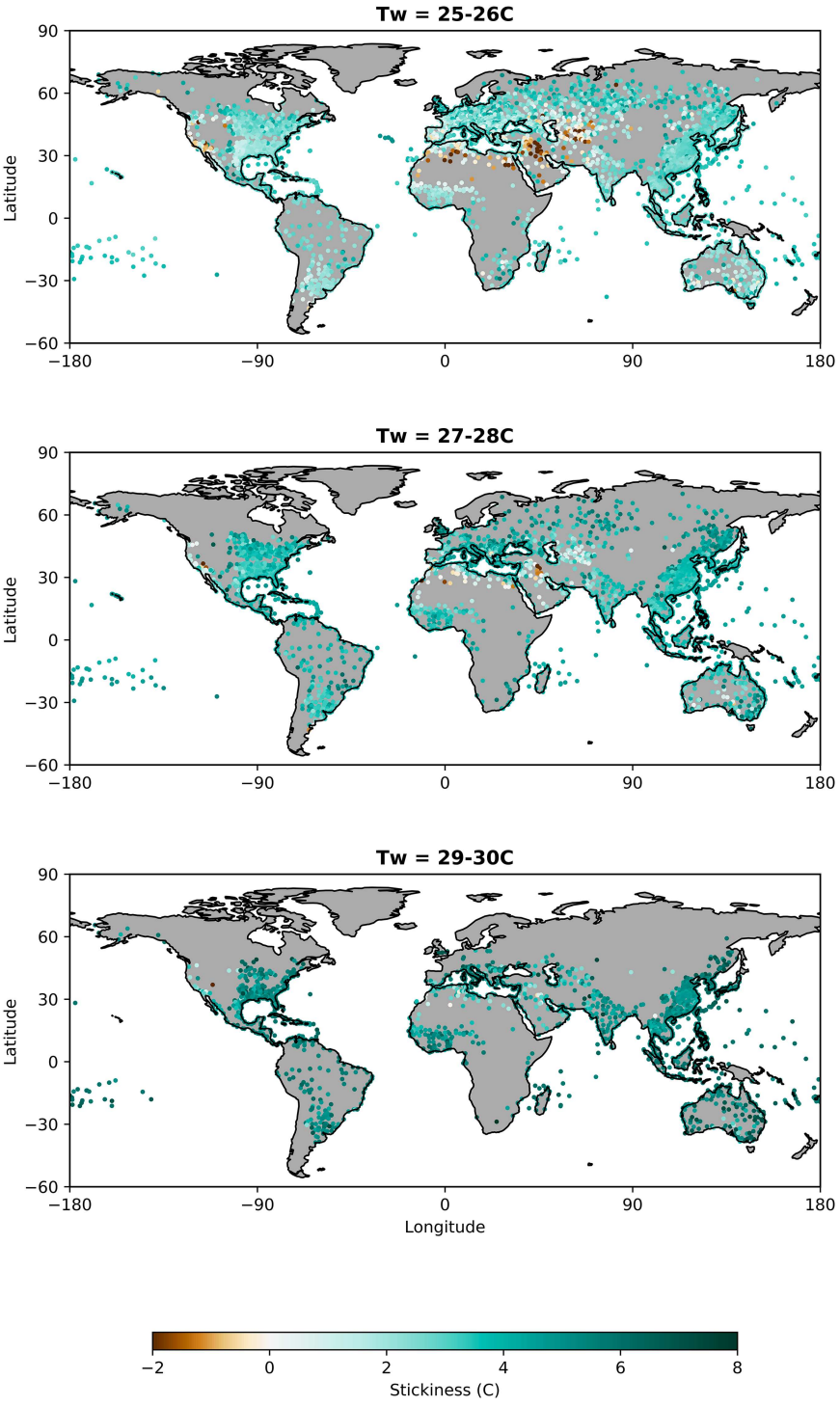

FIG. 10. Mean stickiness conditions during hour of daily maximum T_w of a specific threshold. Station locations are only plotted if the T_w threshold is surpassed in the historical record.

important to local T_w anomalies, in some cases via localized phenomena such as downslope wind events (Gershunov et al. 2021). These patterns may become increasingly important as populous cities at high elevation such as Denver, Colorado, or Kabul, Afghanistan, begin to experience more heat extremes in the future (Coffel et al. 2018).

Stickiness also serves as an efficient and consistent quantitative metric to assess the varying contributions from

temperature and specific humidity toward humid heat events at an individual location over time. The present study highlights the wide variation in the temperature versus humidity contributions to moderate humid heat in many regions, in agreement with regionally specific studies in locations such as the Persian Gulf, South Asia, China, and the United States (Ivanovich et al. 2022; Wang et al. 2019; Raymond et al. 2017). Large scale modes of climate variability such as El Niño Southern Oscillation, the Madden–Julian oscillation, and the boreal summer intraseasonal oscillation have been shown to influence extreme humid heat across the globe (Ivanovich et al. 2022; Speizer et al. 2022) and may contribute to the high variability in stickiness observed in regions such as the Sahel. Variability may also be influenced directly by changes in sea surface temperature, particularly in regions such as South Africa in close proximity to the Agulhas Current (Rouault et al. 2002). In southeast Australia, high variability may be strongly influenced by wind direction on a variety of time scales, whether by synoptic scale disturbances or seasonal monsoon circulation, and associated moisture transport (Watterson 2001).

The capacity of stickiness to quantify the contribution of temperature and specific humidity toward humid heat extremes may help locations identify which variables are most important to predicting the local occurrence of heat stress. There is ongoing debate concerning the physiological expectation that humidity is an important factor for the experience of human heat stress (Mora et al. 2017; Parsons 2006; Steadman 1979; Fanger 1970) versus the lack of epidemiological evidence that high humidity helps to predict human mortality and morbidity compared to dry-bulb temperature alone (Armstrong et al. 2019; Vaneckova et al. 2011; Barnett et al. 2010). One challenge which may contribute to this disagreement is that locations where we might expect a low correlation between extreme dry and humid heat days (i.e., locations where humidity contains the most independent information about humid heat stress compared to dry-bulb temperatures) rarely overlap with locations with available and reliable human health data (Baldwin et al. 2023). Places with high variability in stickiness during local warm periods could point to regions where the differential impacts of extreme dry and humid heat on human health may be more easily separated, should the necessary human health data be available. In regions that exhibit either high variability in stickiness or consistently high stickiness, communicating heat stress risk using a heat stress metric rather than dry-bulb temperature alone may be essential for the most effective local extreme event preparedness. Identifying regions with consistently negative stickiness may also offer insights. In such regions, humid heat extremes tend to be driven by elevated dry-bulb temperatures. Traditional metrics of tracking heat stress based on dry-bulb temperature alone or more temperature-dependent heat stress metrics (e.g., heat index) may be sufficient in these locations to identify future extreme heat stress days. Given that the interpretation of results and translation into adaptation methods depends strongly on the heat stress metric selected (Simpson et al. 2023), introducing stickiness as offering an additional perspective on these disagreements may be helpful, in combination with other metrics. Such explorations using stickiness should also consider the influence of physiological health and climate acclimatization on individuals' experience of heat stress, which can inform regional applications of the variable. Knowing the local shape of the stickiness distribution in a region may also help to forecast when an individual meteorological event may or may not pose a threat of extreme humid heat. For example, in the Persian and Arabian Gulf where humid heat extremes tend to have high stickiness, a high pressure system that increases local temperatures may not be as detrimental as the stalling of summer winds over the Gulf waters which allows for the buildup of moisture along the coast (Ivanovich et al. 2022; Raymond et al. 2021). In the current analysis, we do not differentiate between variability driven by interannual or intra-annual changes and hypothesize that both may play an important role in local stickiness variability.

Distinguishing between humid heat driven by anomalous temperature and humidity through the use of metrics such as stickiness helps to prepare for the unique impacts of each type of extreme. Most heat stress studies have examined T_w above a certain threshold, such as the local 99th percentile or a fixed 35°C value. However, Vecellio et al. (2022) found that for a fixed T_w, humid heat generated by higher dry-bulb temperatures is in fact significantly more dangerous to human health than that by high humidity and moderate temperatures, due primarily to physiological limitations on sweat rates. As a result, identifying locations that experience moderately high T_w and low stickiness, such as the southwest United States, may improve the ability of climate studies to address potential heat stress risks that are not typically identified by considering T_w or other traditional heat stress metrics alone (Simpson et al. 2023; Vanos et al. 2020). Additionally, low stickiness may be worse for plant health due to increased vapor pressure deficit or associated with increased risk of wildfire at high temperatures and low humidity (Ting et al. 2023). Future work could compare stickiness conditions to crop productivity data or wildfire occurrence to test these relationships explicitly. Stickiness variability also affects the local implications for humid heat of practices such as irrigation, which have been shown to increase local humidity conditions and trigger extreme humid heat (Jha et al. 2022; Krakauer et al. 2020; Mishra et al. 2020; Monteiro and Caballero 2019). While irrigation has been shown to reduce local dry heat conditions, the local increases in humidity can often compensate and increase humid heat conditions. Particularly in regions where economic livelihoods depend on agricultural labor, considering current conditions and the possible tradeoffs of these changes is essential.

The potential future extensions of this research range from dynamical to impacts-focused. Here we explore the subseasonal variability of stickiness in each of the case study regions by plotting the full records for the JJA and DJF seasons using daily-scale data. Identifying extreme humid heat events from each of these regions and exploring the temporal evolution of stickiness on hourly time scales could elucidate specific physical mechanisms. For example, tracking the evolution of stickiness throughout the duration of meteorological events such as a thunderstorm while considering the simultaneous influence

of the local background climate, vegetation, and urbanization could shed light upon the physical processes that shape these events and the potential for compound extremes. Future applications of this work could also investigate the modulation of extreme dry and humid heat by vegetation cover. As demonstrated by the distinction between global patterns of stickiness compared to temperature and specific humidity alone, utilizing stickiness could help to evaluate how vegetation cover might influence potential constraints on both dry-bulb temperatures and vapor pressure deficits in locations such as the U.S. Midwest by increasing local surface level moisture. The presence of dense vegetation in this midlatitude region could serve as a mediator to limit extreme dry-bulb temperatures and vapor pressure deficits, helping to buffer any potential threats to crop productivity associated with high canopy dry-bulb temperatures (Mueller et al. 2016). Future work should also explore the influence of dataset uncertainties as well as how stickiness interacts with the nonclimate dimensions of heat stress impacts, such as how access to artificial cooling and the amount of strenuous outdoor activity could shift with heat hazards and stickiness variations. Finally, additional research could attempt extensions to our derivation of stickiness by quantifying the contributions toward humid heat from other climate variables known to influence human health, such as solar insolation and wind speed (Ioannou et al. 2022; Buzan et al. 2015).

As climate change continues to affect land–ocean contrasts and atmospheric circulation, in addition to other factors such as urbanization, deforestation, and agricultural land-use patterns, local stickiness conditions may shift. Further research should consider how future changes in global temperature and moisture patterns will influence the types of humid heat extremes and inform how to best prepare for their distinct societal impacts. In speaking to both atmospheric physics and public health impacts, stickiness provides a uniquely holistic approach for characterizing the spatial and temporal diversity of extreme humid heat events.

Acknowledgments. Funding for C. Ivanovich and R. Horton was provided by National Oceanic and Atmospheric Administration's Regional Integrated Sciences and Assessments program, Grant NA15OAR4310147. A portion of C. Raymond's work was carried out at the Jet Propulsion Laboratory, California Institute of Technology, under a contract with the National Aeronautics and Space Administration (80NM0018D0004). A. H. Sobel acknowledges support from NSF Grant AGS-1933523. The authors declare no conflicts of interest with regard to this research. We thank Marc Spiegelman for his advice on mathematical questions that came up in the derivation of stickiness.

Data availability statement. All datasets used in this analysis are publicly accessible via the following websites: HadISD, https://www.metoffice.gov.uk/hadobs/hadisd/; and ERA5, https://www.ecmwf.int/en/forecasts/datasets/reanalysis-datasets/era5. All code used for the derivations, calculations, and data visualization is publicly available at the following Github repository: https://github.com/ccivanovich/Stickiness.

REFERENCES

Abatzoglou, J. T., and A. P. Williams, 2016: Impact of anthropogenic climate change on wildfire across western U.S. forests. *Proc. Natl. Acad. Sci. USA*, **113**, 11 770–11 775, https://doi.org/10.1073/pnas.1607171113.

Armstrong, B., and Coauthors, 2019: The role of humidity in associations of high temperature with mortality: A multicountry, multicity study. *Environ. Health Perspect.*, **127**, 097007, https://doi.org/10.1289/EHP5430.

Baldwin, J. W., T. Benmarhnia, K. L. Ebi, O. Jay, N. J. Lutsko, and J. K. Vanos, 2023: Humidity's role in heat-related health outcomes: A heated debate. *Environ. Health Perspect.*, **131**, 055001, https://doi.org/10.1289/EHP11807.

Barnett, A. G., S. Tong, and A. C. A. Clements, 2010: What measure of temperature is the best predictor of mortality? *Environ. Res.*, **110**, 604–611, https://doi.org/10.1016/j.envres.2010.05.006.

Bohren, C. F., and B. A. Albrecht, 1998: *Atmospheric Thermodynamics*. Oxford University Press, 402 pp.

Bowman, D. M. J. S., and Coauthors, 2009: Fire in the earth system. *Science*, **324**, 481–484, https://doi.org/10.1126/science.1163886.

Buzan, J. R., and M. Huber, 2020: Moist heat stress on a hotter earth. *Annu. Rev. Earth Planet. Sci.*, **48**, 623–655, https://doi.org/10.1146/annurev-earth-053018-060100.

——, K. Oleson, and M. Huber, 2015: Implementation and comparison of a suite of heat stress metrics within the Community Land Model version 4.5. *Geosci. Model Dev.*, **8**, 151–170, https://doi.org/10.5194/gmd-8-151-2015.

Chakraborty, T., Z. S. Venter, Y. Qian, and X. Lee, 2022: Lower urban humidity moderates outdoor heat stress. *AGU Adv.*, **3**, e2022AV000729, https://doi.org/10.1029/2022AV000729.

Coffel, E. D., R. M. Horton, and A. de Sherbinin, 2018: Temperature and humidity based projections of a rapid rise in global heat stress exposure during the 21st century. *Environ. Res. Lett.*, **13**, 014001, https://doi.org/10.1088/1748-9326/aaa00e.

——, C. Lesk, J. M. Winter, E. C. Osterberg, and J. S. Mankin, 2022: Crop-climate feedbacks boost U.S. maize and soy yields. *Environ. Res. Lett.*, **17**, 024012, https://doi.org/10.1088/1748-9326/ac4aa0.

Dai, A., 2006: Recent climatology, variability, and trends in global surface humidity. *J. Climate*, **19**, 3589–3606, https://doi.org/10.1175/JCLI3816.1.

Davies-Jones, R., 2008: An efficient and accurate method for computing the wet-bulb temperature along pseudoadiabats. *Mon. Wea. Rev.*, **136**, 2764–2785, https://doi.org/10.1175/2007MWR2224.1.

Dunn, R. J. H., 2019: HadISD version 3: Monthly updates. Hadley Centre Tech. Note 103, 10 pp.

——, K. M. Willett, P. W. Thorne, E. V. Woolley, I. Durre, A. Dai, D. E. Parker, and R. S. Vose, 2012: HadISD: A quality-controlled global synoptic report database for selected variables at long-term stations from 1973–2011. *Climate Past*, **8**, 1649–1679, https://doi.org/10.5194/cp-8-1649-2012.

Fanger, P. O., 1970: *Thermal Comfort: Analysis and Applications in Environmental Engineering*. Danish Technical Press, 244 pp.

Flament, P., 2002: A state variable for characterizing water masses and their diffusive stability: Spiciness. *Prog. Oceanogr.*, **54**, 493–501, https://doi.org/10.1016/S0079-6611(02)00065-4.

Gershunov, A., and Coauthors, 2021: Hot and cold flavors of southern California's Santa Ana winds: Their causes, trends, and links with wildfire. *Climate Dyn.*, **57**, 2233–2248, https://doi.org/10.1007/s00382-021-05802-z.

He, Y., X. Zhu, Z. Sheng, and M. He, 2023: Resonant waves play an important role in the increasing heat waves in Northern Hemisphere mid-latitudes under global warming. *Geophys. Res. Lett.*, **50**, e2023GL104839, https://doi.org/10.1029/2023GL104839.

Hersbach, H., and Coauthors, 2020: The ERA5 global reanalysis. *Quart. J. Roy. Meteor. Soc.*, **146**, 1999–2049, https://doi.org/10.1002/qj.3803.

Horton, R. M., J. S. Mankin, C. Lesk, E. Coffel, and C. Raymond, 2016: A review of recent advances in research on extreme heat events. *Curr. Climate Change Rep.*, **2**, 242–259, https://doi.org/10.1007/s40641-016-0042-x.

Im, E.-S., J. S. Pal, and E. A. B. Eltahir, 2017: Deadly heat waves projected in the densely populated agricultural regions of South Asia. *Sci. Adv.*, **3**, e1603322, https://doi.org/10.1126/sciadv.1603322.

Ioannou, L. G., and Coauthors, 2022: Indicators to assess physiological heat strain—Part 3: Multi-country field evaluation and consensus recommendations. *Temperature*, **9**, 274–291, https://doi.org/10.1080/23328940.2022.2044739.

Ivanovich, C., W. Anderson, R. Horton, C. Raymond, and A. Sobel, 2022: The influence of intraseasonal oscillations on humid heat in the Persian Gulf and South Asia. *J. Climate*, **35**, 4309–4329, https://doi.org/10.1175/JCLI-D-21-0488.1.

——, R. M. Horton, A. H. Sobel, and D. Singh, 2024: Subseasonal variability of humid heat during the South Asian summer monsoon. *Geophys. Res. Lett.*, **51**, e2023GL107382, https://doi.org/10.1029/2023GL107382.

Jha, R., A. Mondal, A. Devanand, M. K. Roxy, and S. Ghosh, 2022: Limited influence of irrigation on pre-monsoon heat stress in the Indo-Gangetic Plain. *Nat. Commun.*, **13**, 4275, https://doi.org/10.1038/s41467-022-31962-5.

Kovats, R. S., and S. Hajat, 2008: Heat stress and public health: A critical review. *Annu. Rev. Public Health*, **29**, 41–55, https://doi.org/10.1146/annurev.publhealth.29.020907.090843.

Krakauer, N. Y., B. I. Cook, and M. J. Puma, 2020: Effect of irrigation on humid heat extremes. *Environ. Res. Lett.*, **15**, 094010, https://doi.org/10.1088/1748-9326/ab9ecf.

Lu, Y.-C., and D. M. Romps, 2023: Is a wet-bulb temperature of 35°C the correct threshold for human survivability? *Environ. Res. Lett.*, **18**, 094021, https://doi.org/10.1088/1748-9326/ace83c.

Lutsko, N. J., 2021: The relative contributions of temperature and moisture to heat stress changes under warming. *J. Climate*, **34**, 901–917, https://doi.org/10.1175/JCLI-D-20-0262.1.

Mallya, G., L. Zhao, X. C. Song, D. Niyogi, and R. S. Govindaraju, 2013: 2012 Midwest drought in the United States. *J. Hydrol. Eng.*, **18**, 737–745, https://doi.org/10.1061/(ASCE)HE.1943-5584.0000786.

Masterton, J. M., and F. A. Richardson, 1979: *Humidex: A Method of Quantifying Human Discomfort due to Excessive Heat and Humidity*. Environment Canada, Atmospheric Environment, 45 pp., https://bac-lac.on.worldcat.org/oclc/1032942635.

Matthews, T., 2018: Humid heat and climate change. *Prog. Phys. Geogr.*, **42**, 391–405, https://doi.org/10.1177/0309133318776490.

MacLeod, D. A., H. L. Cloke, F. Pappenberger, and A. Weisheimer, 2016: Improved seasonal prediction of the hot summer of 2003 over Europe through better representation of uncertainty in the land surface. *Quart. J. Roy. Meteor. Soc.*, **142**, 79–90, https://doi.org/10.1002/qj.2631.

Mishra, V., A. K. Ambika, A. Asoka, S. Aadhar, J. Buzan, R. Kumar, and M. Huber, 2020: Moist heat stress extremes in India enhanced by irrigation. *Nat. Geosci.*, **13**, 722–728, https://doi.org/10.1038/s41561-020-00650-8.

Monteiro, J. M., and R. Caballero, 2019: Characterization of extreme wet-bulb temperature events in Southern Pakistan. *Geophys. Res. Lett.*, **46**, 10 659–10 668, https://doi.org/10.1029/2019GL084711.

Mora, C., and Coauthors, 2017: Global risk of deadly heat. *Nat. Climate Change*, **7**, 501–506, https://doi.org/10.1038/nclimate3322.

Mueller, N. D., E. E. Butler, K. A. McKinnon, A. Rhines, M. Tingley, N. M. Holbrook, and P. Huybers, 2016: Cooling of U.S. Midwest summer temperature extremes from cropland intensification. *Nat. Climate Change*, **6**, 317–322, https://doi.org/10.1038/nclimate2825.

Nelder, J. A., and R. Mead, 1965: A simplex method for function minimization. *Comput. J.*, **7**, 308–313, https://doi.org/10.1093/comjnl/7.4.308.

Otkin, J. A., and Coauthors, 2016: Assessing the evolution of soil moisture and vegetation conditions during the 2012 United States flash drought. *Agric. For. Meteor.*, **218–219**, 230–242, https://doi.org/10.1016/j.agrformet.2015.12.065.

Pal, J. S., and E. A. B. Eltahir, 2016: Future temperature in southwest Asia projected to exceed a threshold for human adaptability. *Nat. Climate Change*, **6**, 197–200, https://doi.org/10.1038/nclimate2833.

Parsons, K., 2006: Heat stress standard ISO 7243 and its global application. *Ind. Health*, **44**, 368–379, https://doi.org/10.2486/indhealth.44.368.

Photiadou, C., M. Jones, D. Keellings, and C. Dewes, 2014: Modeling European hot spells using extreme value analysis. *Climate Res.*, **58**, 193–207, https://doi.org/10.3354/cr01191.

Raymond, C., D. Singh, and R. M. Horton, 2017: Spatiotemporal patterns and synoptics of extreme wet-bulb temperature in the contiguous United States. *J. Geophys. Res. Atmos.*, **122**, 13 108–13 124, https://doi.org/10.1002/2017JD027140.

——, T. Matthews, and R. M. Horton, 2020: The emergence of heat and humidity too severe for human tolerance. *Sci. Adv.*, **6**, eaaw1838, https://doi.org/10.1126/sciadv.aaw1838.

——, ——, ——, E. M. Fischer, S. Fueglistaler, C. Ivanovich, L. Suarez-Gutierrez, and Y. Zhang, 2021: On the controlling factors for globally extreme humid heat. *Geophys. Res. Lett.*, **48**, e2021GL096082, https://doi.org/10.1029/2021GL096082.

——, and Coauthors, 2022: Regional and elevational patterns of extreme heat stress change in the U.S. *Environ. Res. Lett.*, **17**, 064046, https://doi.org/10.1088/1748-9326/ac7343.

Rogers, C. D. W., M. Ting, C. Li, K. Kornhuber, E. D. Coffel, R. M. Horton, C. Raymond, and D. Singh, 2021: Recent increases in exposure to extreme humid-heat events disproportionately affect populated regions. *Geophys. Res. Lett.*, **48**, e2021GL094183, https://doi.org/10.1029/2021GL094183.

Röthlisberger, M., and L. Papritz, 2023: A global quantification of the physical processes leading to near-surface cold extremes. *Geophys. Res. Lett.*, **50**, e2022GL101670, https://doi.org/10.1029/2022GL101670.

Rouault, M., S. A. White, C. J. C. Reason, J. R. E. Lutjeharms, and I. Jobard, 2002: Ocean–atmosphere interaction in the Agulhas Current region and a South African extreme weather event. *Wea. Forecasting*, **17**, 655–669, https://doi.org/10.1175/1520-0434(2002)017<0655:OAIITA>2.0.CO;2.

Schauberger, B., and Coauthors, 2017: Consistent negative response of U.S. crops to high temperatures in observations and crop models. *Nat. Commun.*, **8**, 13931, https://doi.org/10.1038/ncomms13931.

Sherwood, S. C., and M. Huber, 2010: An adaptability limit to climate change due to heat stress. *Proc. Natl. Acad. Sci. USA*, **107**, 9552–9555, https://doi.org/10.1073/pnas.0913352107.

Simpson, C. H., O. Brousse, K. L. Ebi, and C. Heaviside, 2023: Commonly used indices disagree about the effect of moisture on heat stress. *npj Climate Atmos. Sci.*, **6**, 78, https://doi.org/10.1038/s41612-023-00408-0.

Speizer, S., C. Raymond, C. Ivanovich, and R. M. Horton, 2022: Concentrated and intensifying humid heat extremes in the IPCC AR6 regions. *Geophys. Res. Lett.*, **49**, e2021GL097261, https://doi.org/10.1029/2021GL097261.

Steadman, R. G., 1979: The assessment of sultriness. Part I: A temperature-humidity index based on human physiology and clothing science. *J. Appl. Meteor.*, **18**, 861–873, https://doi.org/10.1175/1520-0450(1979)018<0861:TAOSPI>2.0.CO;2.

Tan, J., and Coauthors, 2010: The urban heat island and its impact on heat waves and human health in Shanghai. *Int. J. Biometeor.*, **54**, 75–84, https://doi.org/10.1007/s00484-009-0256-x.

Ting, M., C. Lesk, C. Liu, C. Li, R. M. Horton, E. D. Coffel, C. D. W. Rogers, and D. Singh, 2023: Contrasting impacts of dry versus humid heat on U.S. corn and soybean yields. *Sci. Rep.*, **13**, 710, https://doi.org/10.1038/s41598-023-27931-7.

Vaneckova, P., and Coauthors, 2011: Do biometeorological indices improve modeling outcomes of heat-related mortality? *J. Appl. Meteor. Climatol.*, **50**, 1165–1176, https://doi.org/10.1175/2011JAMC2632.1.

Vanos, J. K., J. W. Baldwin, O. Jay, and K. L. Ebi, 2020: Simplicity lacks robustness when projecting heat-health outcomes in a changing climate. *Nat. Commun.*, **11**, 6079, https://doi.org/10.1038/s41467-020-19994-1.

——, G. Guzman-Echavarria, J. W. Baldwin, C. Bongers, K. L. Ebi, and O. Jay, 2023: A physiological approach for assessing human survivability and liveability to heat in a changing climate. *Nat. Commun.*, **14**, 7653, https://doi.org/10.1038/s41467-023-43121-5.

Vecellio, D. J., S. T. Wolf, R. M. Cottle, and W. L. Kenney, 2022: Evaluating the 35°C wet-bulb temperature adaptability threshold for young, healthy subjects (PSU HEAT Project). *J. Appl. Physiol.*, **132**, 340–345, https://doi.org/10.1152/japplphysiol.00738.2021.

Wang, P., L. R. Leung, J. Lu, F. Song, and J. Tang, 2019: Extreme wet-bulb temperatures in China: The significant role of moisture. *J. Geophys. Res. Atmos.*, **124**, 11 944–11 960, https://doi.org/10.1029/2019JD031477.

Watterson, I. G., 2001: Wind-induced rainfall and surface temperature anomalies in the Australian region. *J. Climate*, **14**, 1901–1922, https://doi.org/10.1175/1520-0442(2001)014<1901:WIRAST>2.0.CO;2.

Wright, M., 1996: Direct search methods: Once scorned, now respectable. *Numerical analysis: Proceedings of the 1995 Dundee Biennial Conference in Numerical Analysis*, D. F. Griffiths and G. A. Watson, Eds., Addison-Wesley, 191–208.

Xue, P., and E. A. B. Eltahir, 2015: Estimation of the heat and water budgets of the Persian (Arabian) Gulf using a regional climate model. *J. Climate*, **28**, 5041–5062, https://doi.org/10.1175/JCLI-D-14-00189.1.

Zscheischler, J., and S. I. Seneviratne, 2017: Dependence of drivers affects risks associated with compound events. *Sci. Adv.*, **3**, e1700263, https://doi.org/10.1126/sciadv.1700263.

——, and Coauthors, 2020: A typology of compound weather and climate events. *Nat. Rev. Earth Environ.*, **1**, 333–347, https://doi.org/10.1038/s43017-020-0060-z.